ELSEVIER

International Journal of Heat and Fluid Flow 20 (1999) 128–141

International Journal of HEAT AND FLUID FLOW

Measurement of momentum and heat transport in the turbulent channel flow with embedded longitudinal vortices

Susanne Lau [1], Kerstin Meiritz [2], Venkatesa I. Vasanta Ram *

Institut für Thermo- und Fluiddynamik, Ruhr-Universität Bochum, Gebaude IB 6/43, P.O.B. 102140, Universitatsstrasse 150, D-44780 Bochum, Germany

Received 10 November 1997; accepted 7 October 1998

Abstract

Velocity and temperature measurements have been made in the heated turbulent channel flow with embedded longitudinal vortices. The longitudinal vortices were generated through an array of rectangular shaped winglets. Surveys of the velocity and temperature fields in this flow were conducted with quadruple hot-wire probes that enabled measurement of the instantaneous velocity vector and temperature. From the measurements, components of the Reynolds stress tensor and of the turbulent heat flux vector have been deduced. The experimental data base thus established is critically assessed from a point of view of its meeting the demands made on benchmark data that are sought for evaluation of turbulence models.

Keywords: Heated turbulent channel flow; Longitudinal vortices; Quadruple hot-wire probe; Momentum transport; Heat transport

Notation

A	cross-sectional area of channel
H	semi-channel height
Q	volume flow rate through channel
T	temperature
U_{ref}	reference velocity, defined through $Q = AU_{\mathrm{ref}}$
a	a time-dependent quantity in the flow, eg. u, v, w, T or E_i
$\overline{a}$	the long-time average of the quantity a
a'	fluctuating part of the quantity a
u, v, w	velocity components in the x, y and z directions, respectively
x, y, z	Cartesian coordinates with x in the streamwise direction, y normal to the walls and z in the spanwise direction
u_τ	wall friction velocity
$\dot{q}_{\mathrm{w}}$	wall heat flux
α, β	angles set during probe calibration, see Fig. 5
φ, γ	angles the velocity vector makes with the x and z axes, respectively, see Fig. 5

1. Introduction

A method of enhancing heat transfer in industrial heat exchangers is through the generation of longitudinal vortices embedded in the flow close to the wall. A common engineering device that generates such vortices is an array of winglets on the heat exchanger walls. Considerations of ease of fabrication require the shape of the winglets to be kept simple. They are therefore often either rectangular or triangular. The flow in these devices is characterised by more or less compact regions of helically wound streamlines (longitudinal vortices) surrounded by regions wherein the streamlines are almost straight. Helical shape of the streamlines implies that they are curved in two planes. In contrast, in the surroundings the streamline curvature is restricted to one plane only and even in this plane which is parallel to the channel walls it is rather mild. Since the structure of the turbulence in any flow region is strongly affected by the streamline curvature, the flow in the devices in question, despite the relative simplicity of their geometry, turns out to be extremely complex. The complexity is of such nature and proportion that the flow has not lent itself to treatment through more conventional turbulence models. It is therefore often referred to in the literature as a complex turbulent flow. The measurement of momentum and heat transport in these flows is an important research task and this is the motivation of the work to be reported. Numerical studies of the turbulent flow in a channel with rectangular winglets were conducted by Zhu et al. (1991) and Zhu (1992) who employed a k–ϵ model for closure. Experimental studies of the surface heat transfer in a channel with rectangular winglets were carried out by Riemann (1992). More recently Neumann

* Corresponding author. E-mail: vvr@Lstm.Ruhr-Uni-Bochum.de.

[1] Present address: GHH BORSIG Turbomaschinen GmbH, Bahnhofstraße 66, 46145 Oberhausen, Germany.

[2] Present address: ASCAD, Harpener Heide 7, 44805 Bochum, Germany.

0142-727X/99/$ – see front matter
PII: S0142-727X(98)10052-8

(1997) has experimentally studied both the hydrodynamic and thermal entry flow problem in a channel with periodically arranged vortex generators. In the past decades studies of the flow and turbulence in the turbulent boundary layer, including heat transfer, have been carried out by Cutler and Bradshaw (1993a, b), Eibeck and Eaton (1985–1987), Shabaka et al. (1988), Wroblewski and Eibeck (1991) and Shizawa and Eaton (1992). For some more recent work on this subject wherein the longitudinal vortices are created by an end-wall junction the reader is referred to Xie and Wroblewski (1997) and Praisner et al. (1997). The aim of the present work is twofold. The first is to acquire experimental data on quantities relevant to the modelling of turbulence in this complex flow under well defined experimental conditions of flow and wall heat transfer. The second is to critically examine the acquired data set from a point of view of whether they meet the requirements of being regarded as a bench mark data set. The motivation behind the second is to draw attention to some inadequacies in the current state of the art of experimental techniques for this complex flow.

In the present work experiments have been conducted in a channel flow facility in which an array of winglets of rectangular shape is mounted on one of the channel walls. The wall with winglets is heated with $\dot{q}_w = \text{const}$. Simultaneous measurements of the instantaneous velocity vector and temperature profiles have been done in this flow. A quadruple hot-wire probe of special design was employed for this purpose. From the probe signals the components of the Reynolds stress tensor and of the heat flux vector, quantities that are of interest both for verification of turbulence models and their further development for a complex flow, have been obtained. The time series available from measurement with this probe also permit extraction of structural features of the fluctuating motion that have acquired importance in more recent work on turbulence modelling. For a preliminary account of these studies the reader is referred to Lau and Vasanta Ram (1998).

2. Experimental apparatus and procedure

2.1. The facility

The velocity and thermal measurements were conducted in two identical but separate facilities, referred to in the following as the cold and the heated facility, respectively. This functional separation enabled better control of the thermal conditions during the temperature measurements which was not necessary for velocity measurements. It also facilitated meeting the various engineering requirements that arose when heating is to be installed.

Both the cold and the heated facilities are essentially low-speed channel flow rigs of large aspect ratio (1:18) with air as the working medium. Salient dimensions of both are given in Fig. 1. The nominal channel height $2H$ is 40 mm. The array of rectangular winglets, arranged in a regular period both stream wise and spanwise, was mounted on one of the channel walls in the area shaded grey in Fig. 1. Salient dimensions of the winglet configuration are shown in Figs. 2 and 3. The winglets protruded up to the mid-channel height. This protrusion, although rather large from the point of view of an engineering device for heat-transfer enhancement, was chosen for the present experiments in order to generate longitudinal vortices large enough to be resolvable with our quadruple hot-wire probe. The computer-operated traverse mechanism for probes described in Lau et al. (1993) is installed on the channel wall opposite to the winglets.

The Reynolds number for the experiments, based on the semi-channel height H and the reference velocity U_{ref} was nominally 10 000. U_{ref} is related to the volume flux Q through $Q = AU_{ref}$ where A is the channel cross-sectional area. In the cold facility Q was obtained by Pitot tube measurement of the center-line velocity at an upstream location where the flow was checked to be free from disturbances due to the winglets. Invoking such a procedure for ascertaining Q through a single point measurement of the velocity is based on the shape of the velocity profile being known. This indeed was the case in our experiment as verified by Pitot tube traverses. They showed that the shape of the velocity profile at the said location of measurement was in agreement with the established laws for fully developed channel flow known through published literature, e.g. Townsend (1976), Ch.5. In deducing Q from a single point measurement point of the velocity, the known velocity profile was taken to extend over the entire channel width. Since the value of Q thus ascertained does not account for the finite span of the channel, the value of the Reynolds number might be expected to have been overestimated, but only slightly so since the channel aspect ratio in our experiment has the rather large value of 18:1. In the heated facility this measurement was done by an orifice meter installed far downstream of the winglets at a location conforming to DIN standards. The accuracy of the orifice meter in the velocity range of interest as given by the manufacturers for such an installation is 1%.

For thermal measurements, an electrically conducting thin foil was cemented on to the wall made out of thermally insulating material. Adjustment of the current passed through the foil regulated the heat input into the flow. The heating rate in our experiments was set to 340 ± 1.2 W/m^2. In a separate study in the same facility in which the wall temperature was measured by an infra-red camera, see Neumann (1997), Neumann et al. (1998), the heat loss to the back wall at this set heating rate was estimated to be at 4% which gives the heat input $\dot{q}_w$ into the flow to be 325 ± 1.2 W/m^2. The heating rate set gave rise to a wall temperature of around 10 K above the ambient in the heated facility.

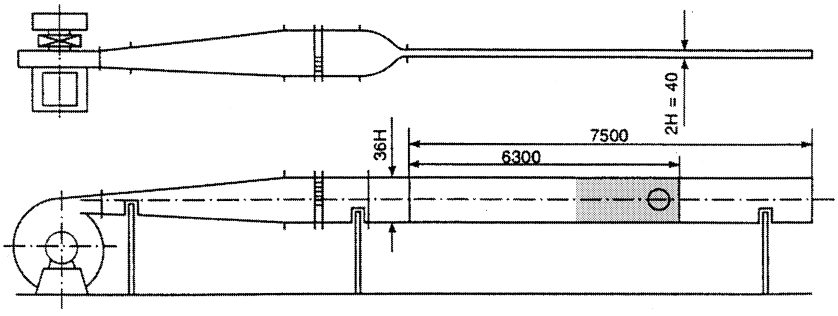

Fig. 1. Channel flow facility. Details of the grey-shaded area on Fig. 3.

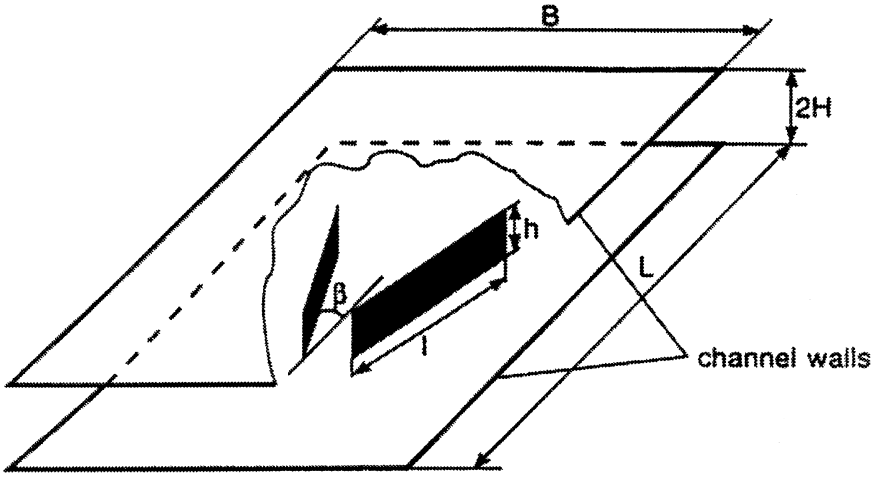

Fig. 2. Periodic element of winglet configuration: geometric parameters of the winglets: $2H = 40$ mm, $L = 200$ mm, $h = 20$ mm, $l = 80$ mm, $B = 160$ mm, $\beta = 30°$.

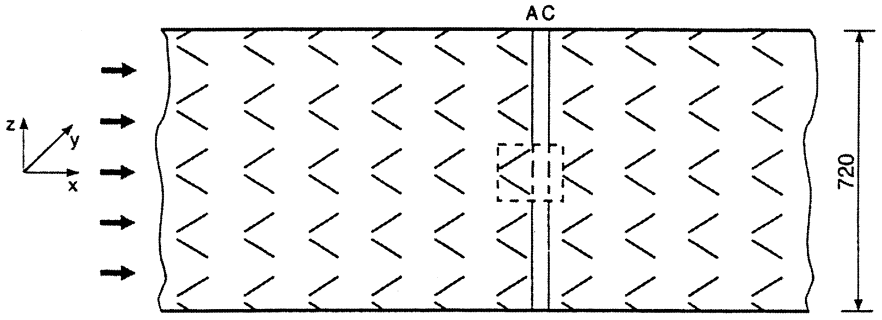

Fig. 3. The grey-shaded area of Fig. 1 showing the periodic winglet configuration with planes of measurement A and C. The square within the dashed lines is a periodic element shown in Fig. 2.

2.2. The quadruple hot-wire probe

The wire arrangement of our quadruple-wire probe is the same as in Eckelmann et al. (1984). It is essentially one in which two X-wire probes are arranged in planes perpendicular to each other, see Fig. 4. The wires are driven independent of each other. The probe, in which the wires are welded on to the prongs, was fabricated in our laboratory. For the vectorial velocity measurements in the cold facility, all the four wires of the probe were of 5 μm diameter, operated in the constant-temperature mode, see Lau (1995). We refer to this probe as Probe Type A. For simultaneous velocity and temperature measurements in the heated facility one pair of diagonally opposite wires of the quadruple wire probe (that make an X-wire probe) were of 5 μm diameter and the other of 2.5 μm diameter. The 2.5 μm wires of the Probe Type B were operated in the constant-current mode with a heating current of 0.3 mA. This probe is referred to as Probe Type B. The driving unit for the quadruple-wire probe of both types A and B was a commercially available anemometer set marketed by AA-Labs, Tel Aviv, Israel.

Tests in our probe calibration facility in which the air temperature could be varied between 20–60°C (see Kostka and Vasanta Ram (1992)) showed that for measurement of the air temperature with the 2.5 μm diameter wires, a heating current of 0.3 mA was an acceptable compromise between the conflicting aims of achieving from the sensor a high signal level and keeping low its sensitivity towards air velocity. With a heating current at this level, no influence of the air velocity on the output signals of the 2.5 μm wires of the Probe Type B was detectable. The 2.5 μm wires thus operated could therefore be regarded as functioning as resistance thermometers in our experiment. Values of the heating current much lower than 0.3 mA, however desirable they might be from the point of view of air-temperature measurement, were not employed in our experiments in view of the unfavourable signal to noise ratio at these settings.

Signals from the pair of 5 μm wires of the Probe type B can, in principle, be processed to evaluate statistical quantities formed with the velocity components in the plane of these wires. The method of evaluation may be found in standard literature on hot wires, e.g. Bruun (1995), Eckelmann (1997). Rewelding the wires on to the prongs with the wire diameters interchanged permitted, again in principle, evaluation of the statistical quantities formed with the velocity components in the plane perpendicular to the previous one.

It is appropriate at this juncture to point out at an inherent limitation of the Probe Type B at simultaneous measurement of velocity and temperature in the complex turbulent flow of the kind in question. The limitation arises primarily since a pair of X-wires operated in the constant-temperature mode cannot resolve the mean velocity components perpendicular to the plane of these wires. It follows therefore that simultaneous measurement of u, v, w and T is not possible with the Probe Type B. The standard methods available in hot-wire literature, e.g. Bruun (1995), only permit evaluating statistical quantities

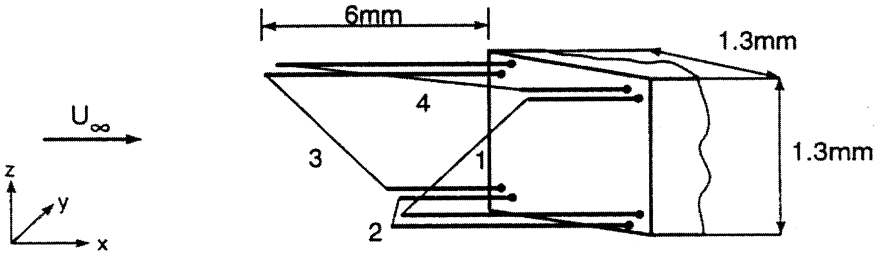

Fig. 4. Quadruple hot-wire probe, lengths not to scale.

formed with velocity components in the plane of the wires, which are one of the sets, either u, v and T or u, w and T. It may therefore appear at first sight that signals from the Probe Type B with the X-pair of constant-temperature wires once in the xy and once in the xz plane, could be employed to evaluate all the components of the Reynolds stresses and the heat-flux vector. However this is not so, which becomes clear on recalling the foundation upon which the evaluation method for the X-probe rests, viz. that the mean velocity lies in the plane of the wires. In the flow with embedded longitudinal vortices it is not possible to meet this requirement everywhere in the flow field during measurement, which in turn leads to errors. Questions concerning errors arising from evaluation of data measured with such probes have to be properly addressed for the data to be suitable as a benchmark.

In the flow surveyed with probes operated in the said manner there is a certain redundancy in measurement of several flow quantities. While it is immediately obvious that the flow quantity measured with the highest degree of redundance is u, there is some redundancy in the measurement of some components of the Reynolds stress tensor too, since the low heating in our experiment may not be expected to affect the fluid motion. Readings from the probes of types A and B can each be evaluated to yield the Reynolds stresses and these can be compared with each other. Such a comparison provides a useful indication of the error caused by the use of a probe not adapted to the flow situation. It thus serves to answer the question just posed, i.e. to test the validity of the assumptions underlying the steps in the evaluation procedure. Since redundant measurements of a flow quantity with two probes are the exception rather than the rule the comparison would enable one to gain an estimate on the magnitude of the errors possible in data acquired through such probes in similar flow situations. Since, when evaluating turbulence models, it is meaningless to expect a prediction accuracy over that achievable in measurement, the measurements with redundancy act as a guide through data. We will enter into a discussion of this point later in Section 5 of this paper.

2.3. Probe calibration, characteristics and use

2.3.1. Flow field

Fig. 5 is a schematic representation of our calibration facility, for details of which we refer to Schulz (1989). The quadruple hot-wire probe was calibrated for its behaviour with respect to the velocity vector. During calibration the temperature in the calibration facility was kept constant and close to the air temperature during measurement which was 33 ± 0.5°C. For this reason no temperature corrections for velocity measurement were necessary. During measurement, the four analogue sensor signals from the quadruple hot-wire probe were digitised by passing them through a DAS20 A/D-converter of 12-bit resolution and the accompanying sample-and-hold box (marketed by Keithley Instruments), and recorded for a duration of 2.5 s. The A/D-converter was installed in a 386 MS-DOS computer, while the sample-and-hold box was external. 5000 samples per channel were acquired at a sampling rate of 2000 Hz.

A feature of the calibration facility that is of importance to data reduction is that the adjustment of the angular position of the probe during calibration is by the setting of the angles α and β (see Fig. 5) which are different from the angles φ and γ that the velocity vector makes with the x- and z-axes of a Cartesian coordinate system. The step in the calibration procedure of obtaining voltages versus velocity was repeated for 169 pairs of (α, β)-angles within a cone of semi-apex angle of 28°. The entire family of calibration curves, hot-wire voltage E_i versus velocity U for each wire, $i = 1, 2, 3, 4$, then forms a hypersurface. E_i can formally be written as $E_i = E_i(\alpha, \beta, U_\infty)$, where α, β are the angles in Fig. 5. Alternatively, E_i may also be written as $E_i = E_i(\varphi, \gamma, U_\infty)$. Examination of the calibration data showed that, while the voltage versus velocity for any pair (α,β) followed a power law, the cosine function after Jorgensen often used in hot-wire work failed to capture the angular characteristics of the probe over the entire expected range in measurement in the present flow. In order to circumvent this source of uncertainty in measurement, it was decided to develop a computer readable look-up table scheme for purposes

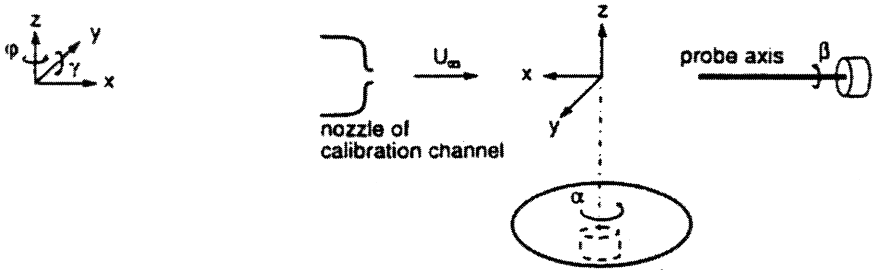

Fig. 5. Schematic diagram of the calibration facility.

of vectorial velocity measurement with the quadruple-wire probe. There are two major steps in this scheme, viz.

1. Generation of a look-up table with a sufficiently high resolution, and
2. development of a search algorithm to assign the velocity components to the quadruple set of measured hot-wire signals.

These will be described in some more detail further in this section.

A look-up table, with a resolution much higher than in the straightforward calibration, was generated by using a priori experimentally verified functional relationships between the hot-wire signals and the three-dimensional velocity vector as seen by the probe. The structure of the functional relationships is sketched later in this section. The search algorithm is based on matching of signals from *all the four wires* to within a specified error in each voltage to determine *the three components* of the velocity vector. This results in a certain redundancy in the u-component which may be expected to lead to a higher accuracy in measurement. An alternative would be to match signals from only three of the four wires to determine the three velocity components and repeat this for different triple-sets of wires. The authors found that for our probe, with its prong and wire configuration, the alternative is not superior since it did not always permit over the entire range a unique inversion of the calibration data to measurement providing at the same time a simple method to estimate the possible error.

2.3.2. Step 1: Generation of the look-up table

The straightforward look-up table would start with about 2535 $(=169\times 15)$ velocity vectors and the corresponding quadruple set of hot-wire voltages, E_1, E_2, E_3, E_4. The arrays of these seven quantities are sorted with respect to the magnitude of the voltages with a given sequence of the different wires. The following fourth order polynomial for voltages vs. velocity magnitude was found to fit the calibration data for any (α,β), so that calibration at 15 values of the velocity magnitude was found to be sufficient.

$$U = C_{1i} + C_{2i}E_i + C_{3i}E_i^2 + C_{4i}E_i^3 + C_{5i}E_i^4, \quad i = 1,2,3,4.$$

From the fourth order polynomial, voltages for any intermediate magnitude of velocity could be obtained through interpolation. For the dependency of the signals on the pair of angles, the hot-wire voltages were interpolated linearly. The final look-up table contains about 287 000 velocity vectors with the corresponding quadruple set of hot-wire voltages, E_1, E_2, E_3, E_4. It should be noted here that, to obtain the velocity components in the Cartesian coordinate system, conversion from (α,β) to $(\varphi,\ \gamma)$ is necessary. Also, even after increased resolution through interpolation, the look-up table is not equally spaced, neither in (u, v, w) nor in (E_1, E_2, E_3, E_4), but this is not a disadvantage as such.

2.3.3. Step 2: The search algorithm

The second step is assigning the components of the velocity vector to the quadruple of voltages. The algorithm developed for this purpose is given in Lau (1996), see also Lau and Vasanta Ram (1998). Matching the quadruple of voltages in measurement to the quadruple in the look-up table to within the specified error in each voltage generally led to more than just one set of possible velocity components. The non-uniqueness of inversion in these cases was handled by chosing the set of velocity components according to the criteria of least square error. This set was then recorded on a file. When no

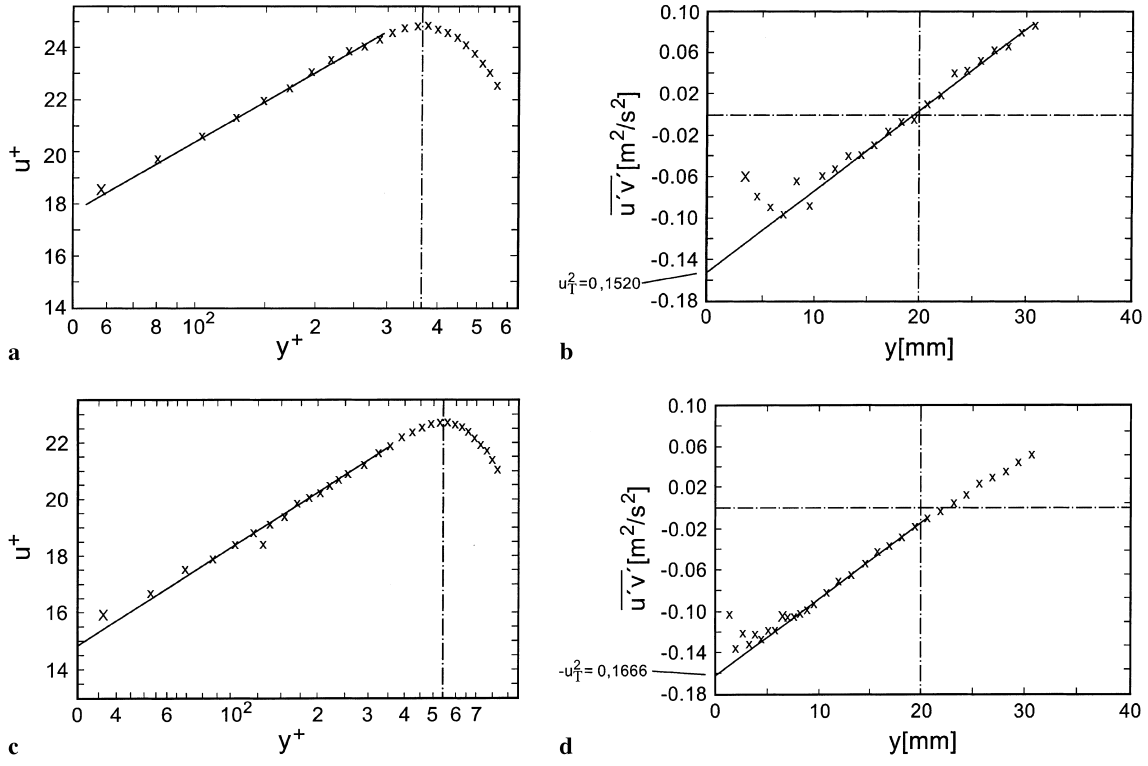

Fig. 6. Undisturbed channel flow. (a) Mean velocity, measurement by Probe Type A. $u^+ = \overline{u}/u_\tau$, $y^+ = yu_\tau/\nu$. u_τ from Fig. 6 (b), $u_\tau = 0.39$ ms^{-1}. The straight line shows a slope of 1/0.38. $-\cdot-\cdot-$ shows location of channel center. (b) Reynolds shear stress $\overline{u'v'}$, measurement by Probe Type A. (c) Mean velocity, measurement by Probe Type B. $u^+ = \overline{u}/u_\tau, y^+ = yu_\tau/\nu$. u_τ from Fig. 6 (d), $u_\tau = 0.408$ ms^{-1}. The straight line shows a slope of 1/0.37. $-\cdot-\cdot-$ shows location of channel center. (d) Reynolds shear stress $\overline{u'v'}$, measurement by Probe Type B.

matching of the quadruple set of voltages in measurement with one in the look-up table was possible the measurement at this instant of time was discarded.

The procedure involving the steps of calibration and use of the quadruple-wire probe was put to test by measuring the profiles of mean velocity $\overline{u}$ and the Reynolds stress $\overline{u'v'}$ and $\overline{u'w'}$ in the fully developed turbulent channel flow free of any disturbances. The plots in Fig. 6(a)–(d) are extracts from the results of such a test. They show profiles of the mean velocity $\overline{u}$ referred to the wall-friction velocity u_τ and of the Reynolds stress $\overline{u'v'}$. The value of the wall friction velocity for these plots has been obtained from extrapolation of the $\overline{u'v'}$ profiles to the wall. The plots, Fig. 6(a) and (c), show the mean velocity profiles to be well captured by both types of probe. The $\overline{u}$-distribution is in accordance with the well-established laws for fully developed turbulent flow in a channel. A more rigorous test of the probe is whether it can capture the Reynolds stress profiles. The plots in Fig. 6(b) and (d) show this to be satisfactory in the mid-region of the channel, the values of the wall-friction velocity obtained by extrapolation of $\overline{u'v'}$ up to the wall agreeing with each other to within 10%. There is a slightly larger scatter in the measurements of Probe Type A, that, we believe, is attributable to the algorithm. Such a scatter is not evident in the results of Probe Type B, which it should be noted, employs conventional and well-tested data reduction procedures. Values of the Reynolds stress of wall distances closer than 6 mm are, it is seen, not reliable.

A recent article in which a four-sensor hot-wire probe, together with a look-up table procedure for calibration and measurement is tested in pipe flow is by Wittmer et al. (1998).

2.3.4. Thermal field

For the combined temperature and velocity measurements the quadruple hot-wire probe of the type B (with two cold wires) was calibrated in two steps. The cold wires were first calibrated for temperature in the range from 20°C to 50°C. The thermal calibration facility for this purpose consisted of a box immersed in a thermal water bath. The water temperature could be held constant to within 0.06 K at several discrete levels. The box contained the probe and a reference Pt 100 thermometer. Since the sensor input-output relationship was found to be linear, calibration at three temperatures was regarded sufficient.

In the second step the probe was calibrated with respect to the velocity vector in a plane only within a wedge of semi-angle 30° in the calibration facility referred to earlier. For the angle $\alpha = 0°$ the calibration for velocity was repeated at three temperatures with the cold wires used as thermometers.

The calibration method uses a linear relation for the instantaneous temperature and the cold-wire signals with different reduction parameter for the wires as suggested by Meyer (1994) and Klick (1992), and the method of Browne et al. (1989) for the two-dimensional velocity vector. The findings of these authors regarding probe characteristics were supported by our experiments. For further details the reader is referred to Lau (1996), Lau and Vasanta Ram (1998).

The response of the cold wire to temperature fluctuations was ascertained by subjecting the probe (wire and prongs) to a step jump in temperature and measuring the time constant in the exponential decay of resistance. The time constant τ_w was of the order of 1 ms which, according to the formula

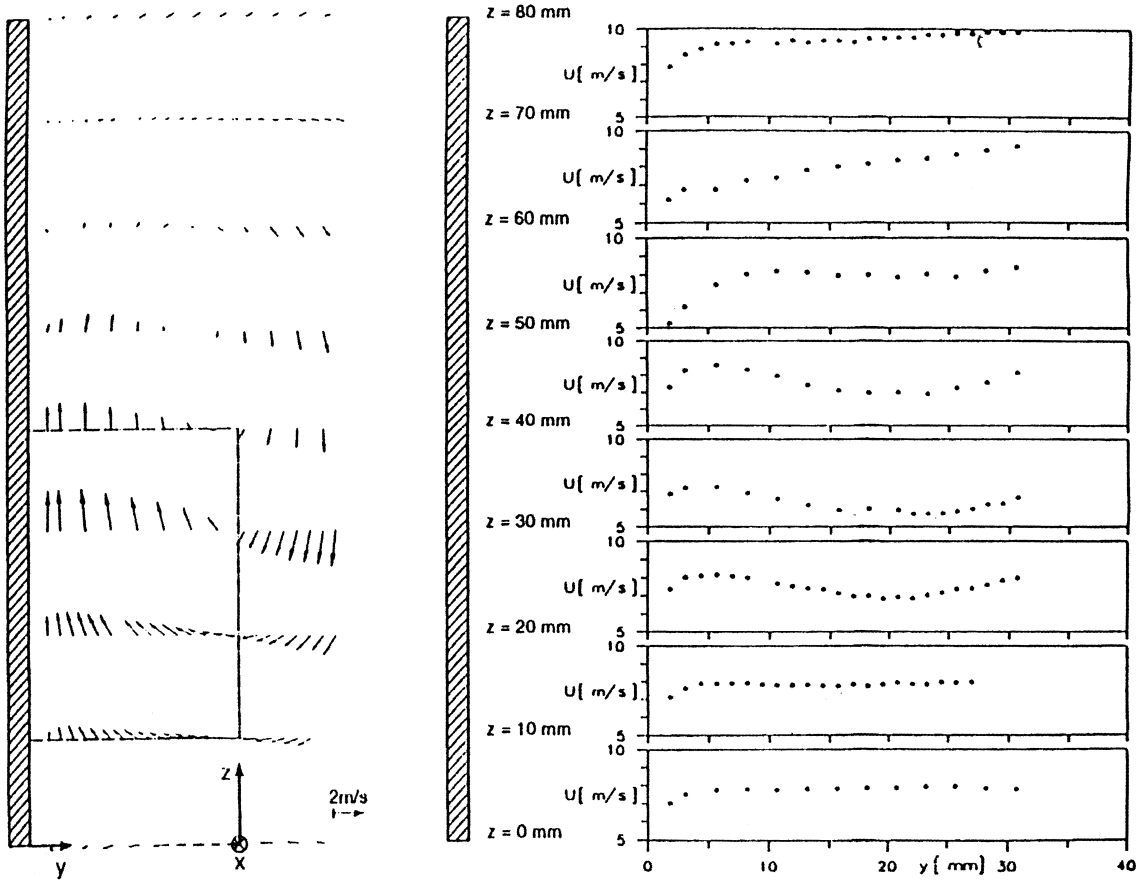

Fig. 7. Secondary and streamwise velocities in the measurement plane C.

$f_c = 1/1.3\tau_w$ (vide Bruun (1995), Eq. 2.55) is equivalent to a cut-off frequency f_c of 0.75 kHz.

3. Measurements

All measurements were done after a steady state was reached. Flow surveys with the probe were conducted in the two planes A and C of Fig. 3 which are 41 and 107 mm respectively downstream of the trailing edge of the winglet. Since, for reliability of measurement with the quadruple hot-wire probe, the velocity vector has to lie within the calibration cone at all instants of time, the measurements were conducted in two runs. In the first run, which we call the preliminary run, an X-wire probe was employed to provide an estimate for the angle the local mean-velocity vector makes with the main-stream (x-)direction in the plane parallel to the channel walls (xz-plane). In the second run, which we call the measurement run, the quadruple hot-wire probe was aligned in the xz-plane with the local mean-velocity vector estimated in the preliminary run. This procedure, although a little tedious, was found to be necessary to acquire reliable instantaneous flow data from the signals of the probe. The final data obtained are then in the form of discrete time series of the instantaneous velocity and temperature.

4. Results

Due to limitations of space we restrict ourselves herein to presenting only a sample selection of results. They will be of some chosen quantities that are of immediate interest in a

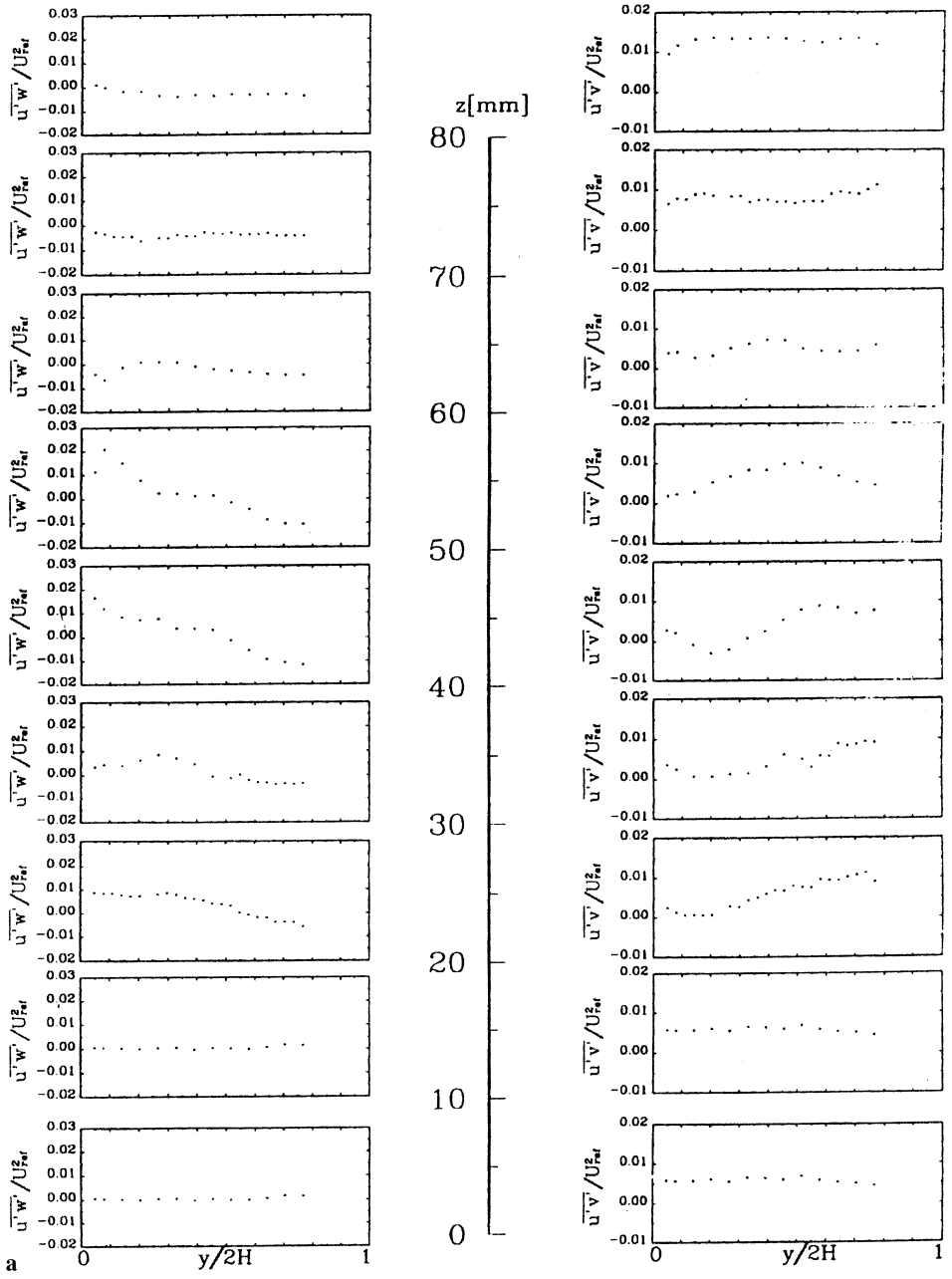

Fig. 8. Reynolds shear stresses $\overline{u'v'}$ and $\overline{u'w'}$ in plane C. (a) Measurement with quadruple wire Probe Type A. (b) Measurement with quadruple wire Probe Type B.

majority of engineering applications. They are presented as plots showing the distribution of the long-time averages of the velocity components $\overline{u}, \overline{v}, \overline{w}$, and the following correlations of fluctuating quantities mostly in the plane C of Fig. 3: the Reynolds stresses $\overline{u'v'}$ and $\overline{u'w'}$, the turbulent kinetic energy k, the Reynolds normal stresses $\overline{u'^2}$, $\overline{v'^2}$, $\overline{w'^2}$, the square of the temperature fluctuation $\overline{T'^2}$ and the temperature–velocity correlations $\overline{v'T'}$ and $\overline{w'T'}$. Our choice of these quantities has been prompted by the aim of many turbulence models being to compute the long-time averages satisfactorily. For further details, in particular of studies of structural features of the fluctuating velocity and temperature fields, the reader is referred to Lau (1995, 1996).

In Fig. 7 the secondary velocity components $\overline{v}$ and $\overline{w}$ are shown as vectors. The longitudinal vortex region is identifiable in this plot through the secondary velocity components being non-zero. This figure also shows that the primary velocity component $\overline{u}$ has a wake-like behaviour in the vortex region. Figs. 8 and 9, parts of which are taken from Lau (1995, 1996), are plots of quantities associated with the velocity fluctuations. Fig. 8(a) and (b) shows the measured Reynolds shear stresses $\overline{u'v'}$ and $\overline{u'w'}$ measured by probes of the type A and B, respectively. We have given in Fig. 8(a) the Reynolds stresses in a dimensionless form to enable a more ready comparison of the characteristic numerical orders of magnitude the quantities assume in this flow with other kinds of complex turbulent flow for which corresponding quantities are available in published literature. The velocity of reference is $U_{\text{ref}} = 8.2\ \text{ms}^{-1}$ that goes with the Reynolds number of 10 000 formed with the semi-channel height H. It may be recalled here that the hot-wire

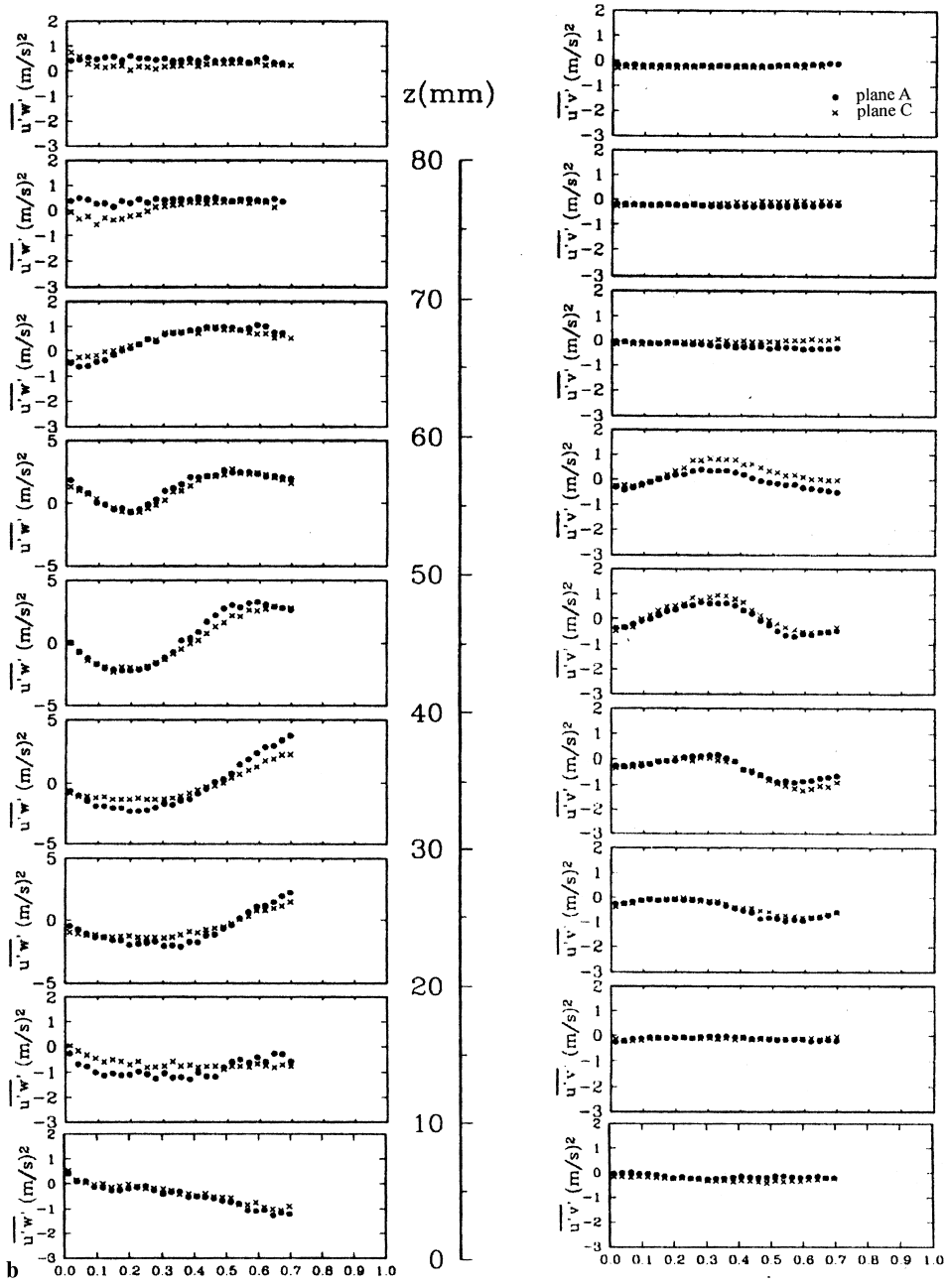

Fig. 8. (Contd).

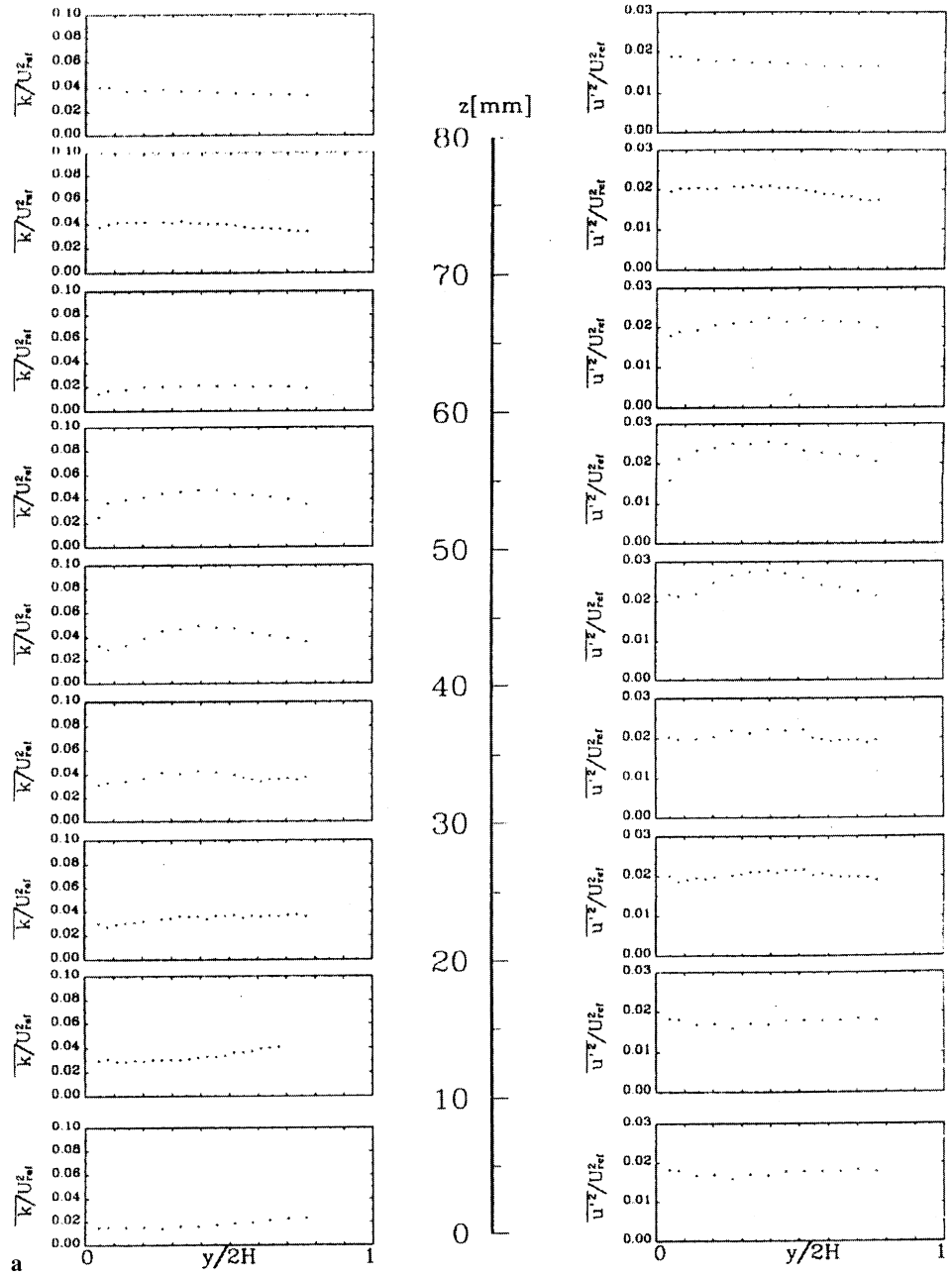

Fig. 9. (a) Turbulent kinetic energy k and Reynolds normal Stress $\overline{u'^2}$ in plane C. Measurement with Probe Type A. (b) Reynolds normal stresses $\overline{v'^2}$ and $\overline{w'^2}$ in plane C. Measurement with Probe Type A.

sensors of the probe type B form an X-probe which yields in principle $\overline{u'v'}$ or $\overline{u'w'}$ depending upon the orientation of the plane containing the hot wires, the xy- or xz-plane. However, since there is a velocity component perpendicular to the plane of the X-wires existent in this flow, the values of the Reynolds stresses $\overline{u'v'}$ and $\overline{u'w'}$ evaluated from the probe type B have to be regarded with some reservation. We will return to this topic in Section 5 of this paper. Fig. 9 shows the turbulent kinetic energy k and the Reynolds normal stresses $\overline{u'^2}$, $\overline{v'^2}$ and $\overline{w'^2}$. Figs. 10 and 11 are plots showing features of the thermal field. Fig. 10 shows that $\overline{T'^2}$ has a maximum of 0.48 K^2 in the vortex core. Fig. 11(a) and (b) show the velocity–temperature correlations $\overline{v'T'}$ and $\overline{w'T'}$. These are seen to be zero at the spanwise locations $z = 0$ mm and $z = 10$ mm which, as a comparison with Fig. 7 would show, lie outside the longitudinal vortex.

5. Discussion

It is known from hitherto published literature (see e.g. Bradshaw (1997)) that turbulence models in wide use at present are not very satisfactory for the class of complex turbulent flows in question. Pinning down the reasons and finding remedies for this shortcoming are goals pursued vigorously at present in ongoing research. An important step in this effort is comparing the values of the terms evaluated from measurements in the budgets of the turbulent kinetic energy and of the various Reynolds stress components with their computed counterparts. However, such a comparison of the budgetary contributions of these quantities has to be carried out judiciously, with due regard to the limitations of the measurement. Since, in our present work, redundant measurements in several

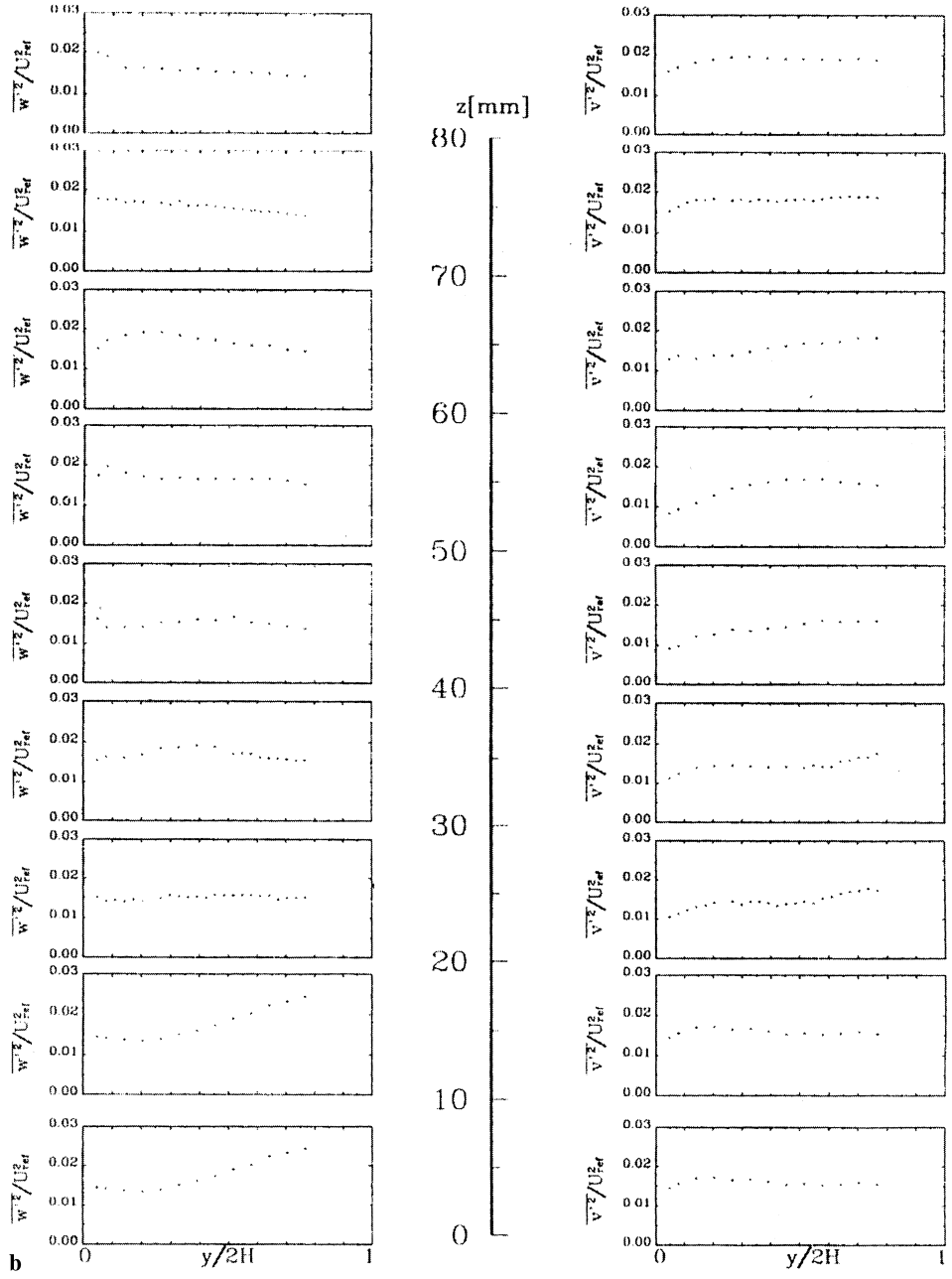

Fig. 9. (Contd).

quantities are available, it is attractive to try to use this information to get an idea of limitations in the interpretation of measured data, and in particular where the limitations are most severe. This is tantamount to addressing the question as to whether the experimental data base is qualified to serve as a benchmark for evaluating turbulence models.

A discussion of the present experiments along this course is, the authors contend, more meaningful than, say, the evaluation of any one specific turbulence model as such. The justification is that, given the state of the art in measurement and the common occurrence of such flows in engineering, the perspective thus gained is of a broader applicability. The critical examination that follows, besides showing up the expected limitations arising from the probe as such, exposes another equally serious determining factor that is known in principle but does not seem to have drawn the attention it deserves in many studies of complex turbulent flows with multi-sensor hot-wire probes. That is what may be called an improper matching of the measuring technique to certain dominant characteristics of the investigated flow field.

The data from our measurements, available in the form of discrete time series of the three velocity components and temperature in the flow field, are processable in principle to yield contributions from most of the terms entering the budgets of the turbulent kinetic energy and the Reynolds stresses. The contribution arising from correlations with pressure fluctuations is however not measurable. Among the rest of the terms, the ones holding particular interest in the context of turbulence modeling would be the triple correlations of the velocity fluctuations, the production of the turbulent kinetic

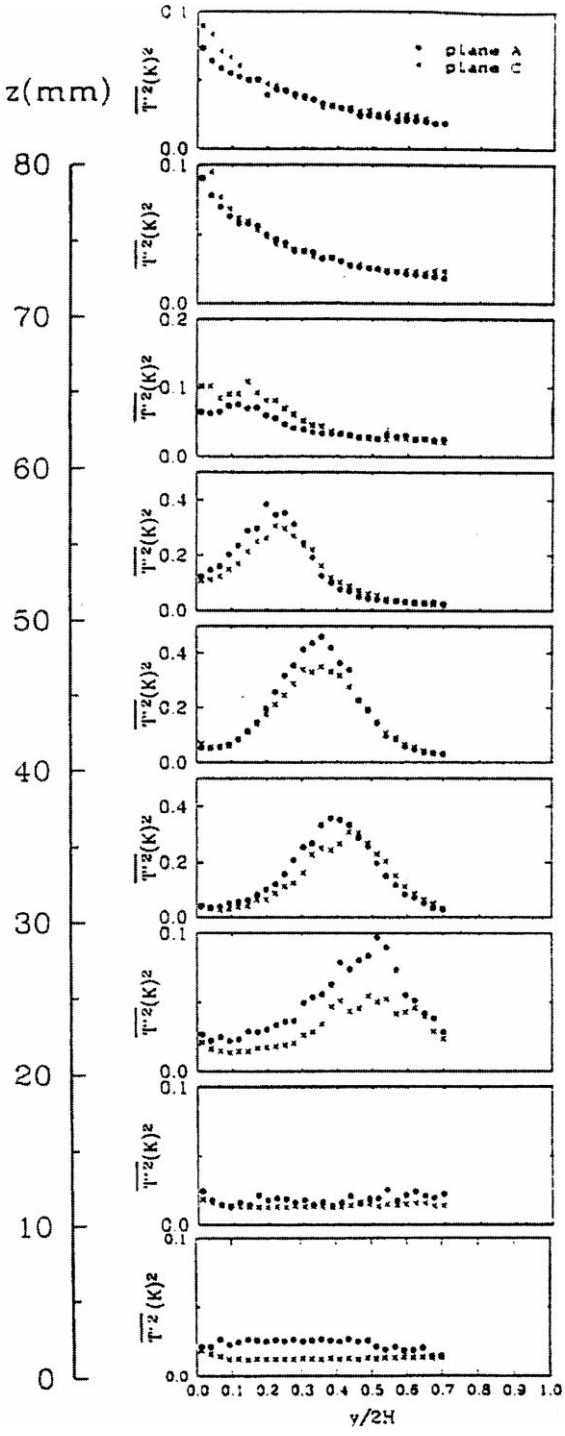

Fig. 10. Square of temperature fluctuations in planes A and C. Measurement with Probe Type B.

energy and of the various Reynolds stress components and similar quantities involving temperature. In this paper we confine our attention to the turbulent kinetic energy k, the Reynolds stresses and the components $\overline{v'T'}$ and $\overline{w'T'}$ of the heat-flux vector. At this juncture it is in order to point out that, in the flow under study, relatively larger errors than in more conventional flows are to be expected in the numerical values of production of the turbulent kinetic energy or of the Reynolds stresses deduced from experimental data. To some extent the source of the error may be traced back to the measurement procedure. The technical requirements of data storage and traversing the probe in the flow geometry made it almost mandatory in this work to space the measuring points less densely in the spanwise direction than in the direction normal to the walls. We observe that this is almost the rule followed in many other experimental studies too. Whereas such a spacing is justifiable in a (conventional) flow in which gradients normal to the wall are much larger in magnitude than in the spanwise direction, in the flow under study it is not everywhere so. As a result, the error in production terms deduced from measurements by replacing derivatives with differences will be relatively large, more particularly so in the region of the vortex.

A cursory inspection of Figs. 7–11 suffices to recognise the region of the longitudinal vortex as the critical one for measurement. It is in this compact region 10 mm $< z <$ 60 mm where the spanwise velocity component $\overline{w}$ changes sign as one proceeds away from the channel wall and the profile of the stream wise velocity component $\overline{u}$ changes in character from "wake-like" to "channel-flow-like". The measured value close to zero of the component $\overline{u'w'}$ of the Reynolds shear stress over the entire channel height at the spanwise location of $z = 0$ in Fig. 8(a) is consistent with the expectation of flow symmetry in this geometry. However, it is worthy of note that this symmetry property does not show up this decisively when the same quantity at the same location is measured by the probe of type B, see Fig. 8(b). It is clear that it is not within the reach of the X-wire arrangement in the probe of type B to measure $\overline{u'w'}$ in the presence of instantaneous v-components as large as in this flow. We also wish to draw attention to the qualitative differences in the profiles of the Reynolds stresses measured by probes A and B. These are rather pronounced in the vortex region. A rough idea of the magnitude of the v-component may be obtained from the plot of $\overline{v'^2}$ in Fig. 9(b).

The other differences in the profiles of $\overline{u'v'}$ and $\overline{u'w'}$ measured by probes of the type A and B in Fig. 8(a) and (b) are possibly ascribable to the same reason viz. that the X-probe may not capture the Reynolds stress components in the plane of the wires to a sufficient accuracy when velocity components perpendicular to this plane affect cooling significantly. Again for the same reason the values $\overline{v'T'}$ and $\overline{w'T'}$ measured by the probe type B and presented in Fig. 11 are open to question. Despite this reservation the data evaluation from this probe gives an idea of the effect of fluctuations on scalar transport. The similarity of profile shapes at the stations A and C both of the temperature fluctuations $\overline{T'^2}$ and the transport terms $\overline{v'T'}$ and $\overline{w'T'}$ indicates that there are regions within the vortex that are convection dominated over this length $x/H = 3.3$ and regions where this is not so.

6. Conclusions

The extraordinary complexity of the channel flow with embedded longitudinal vortices is caused by the rapid changes that both the mean and the fluctuating quantities undergo across the vortex. The Reynolds stresses and the strain rate exhibit large gradients with respect to both magnitude and axis orientation. As a result, a proper resolution of this flow in experiment calls for instrumentation techniques better adapted to these conditions than, say, conventional hot-wire techniques presently available on a commercial scale arc. The quadruple hot-wire probe with its inherent redundancy in measurement appears to hold the promise of meeting this requirement for the velocity field. But, in its present state of the art, a further reduction of size and improvements in efficiency at data handling are essential for it to be usable as a measurement tool in the flow with the small-sized longitudinal vortices that are of

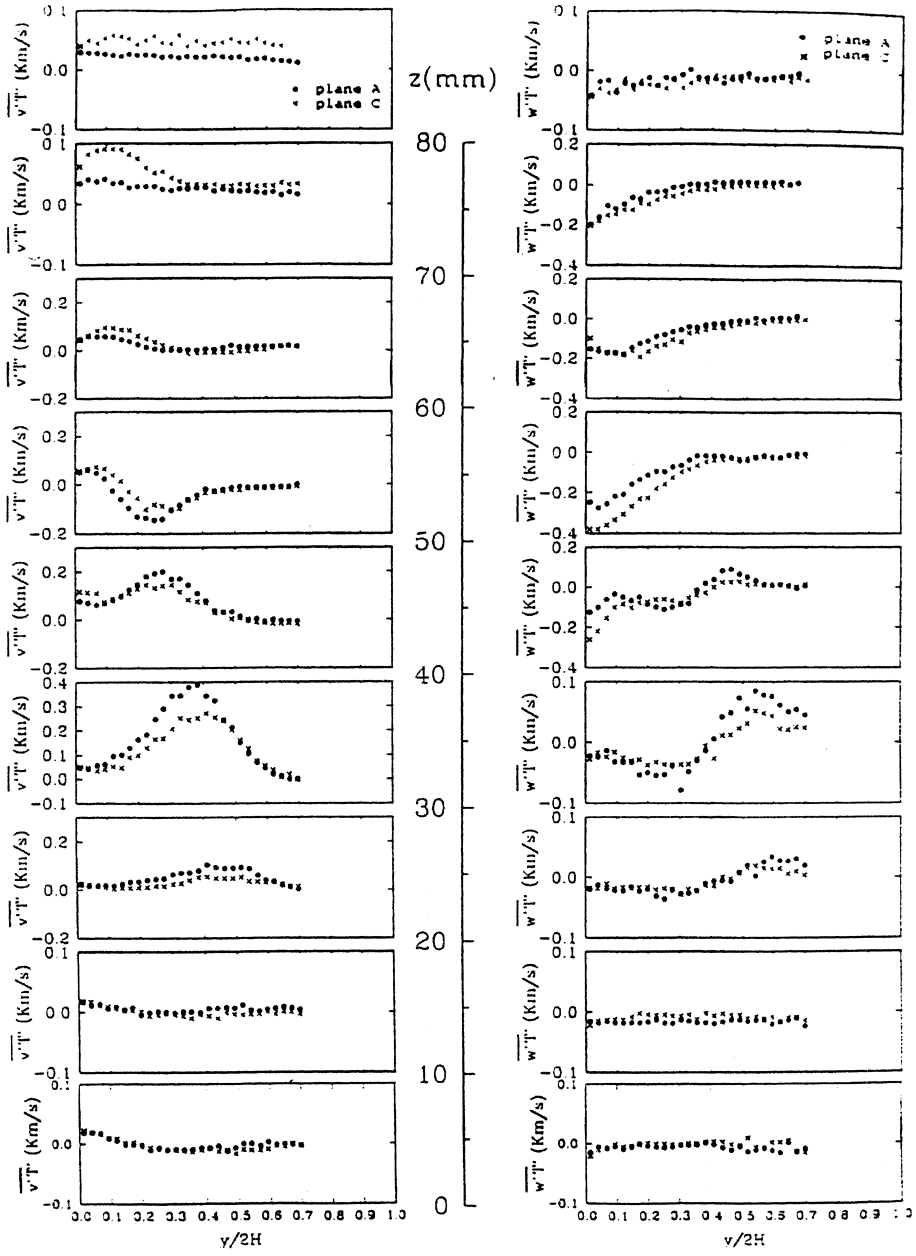

Fig. 11. Velocity–temperature correlations $\overline{v'T'}$ and $\overline{w'T'}$ in planes A and C. Measurement with Probe Type B.

primary interest in heat-exchanger applications. For the measurement of the turbulent thermal transport quantities in the heated flow with embedded longitudinal vortices, simultaneous temperature and velocity measurement through multi-sensor probes based on the X-wire principle for velocity measurement does not provide results of reliability comparable to their velocity counterparts.

Acknowledgements

The authors thank the Deutsche Forschungsgemeinschaft (DFG) for a grant of financial support for this work, Prof. M. Fiebig for providing the heated channel-flow facility and Mr. M. Kaniewski for his help at data reduction and preparation of Fig. 6.

Appendix A. Error estimation

There are several sources of error which are important for estimating measurement uncertainties. They may be traced to the calibration of the quadruple hot-wire probe with respect to temperature and the three-dimensional velocity vector, and to the algorithms that assign the velocity vector and the temperature to the signals from the hot and cold wires of the probe.

In the estimation of uncertainties in velocity measurement, two main sources of error may be identified as important. They are traceable to the calibration of the quadruple hot-wire probe and to the use of the look-up table scheme.

Calibration of the probe is subject to the following errors: The error in setting the angles α and β, as defined in Section 2, is estimated to be $\pm 0.5^\circ$ with respect to the aligning of the probe in the free stream, that in the total pressure in the

calibration facility for determining the velocity 0.1% and in the temperature $\pm 0.5^{\circ}$C. Since the probe was calibrated at the same air temperature as during measurement, the temperature dependency of the signals could be mostly kept small, see Kostka and Vasanta Ram (1992) and Vasanta Ram (1992). The uncertainty at using the 12-bit A/D-converter in the sample and hold mode is 2 bit.

For generating the look-up table, the error of the polynomial fit was checked to be within 0.1% whereas the uncertainty at interpolation of the angles α and β in the table was found to have a maximum of 1° at the most. Since the transformation from (α, β) to (φ, γ) is highly non-linear, the final uncertainty in the velocity components depends upon the region of the calibration domain. Gradients in the flow generally lead to an additional error, whose magnitude is difficult to estimate, see Park and Wallace (1992) and Antonia et al. (1994). On the whole, as Cutler and Bradshaw (1993a, b) observe, it is not meaningful to estimate the uncertainty in an experiment such as the present one through application of more conventional procedures, such as e.g. proposed by Kline (1985) and Moffat (1985).

References

Antonia, R.A., Zhi, Y., Kim, J., 1994. Corrections for spatial velocity derivatives in a turbulent shear flow. Experiments in Fluids 16, 411–413.

Bradshaw, P., 1997. Understanding and prediction of turbulent flow – 1996. International Journal of Heat and Fluid Flow 18 (1), 45–54.

Bruun, H.H., 1995. Hot-Wire Anemometry. Oxford University Press, Oxford.

Browne, L.W.B., Antonia, R.A., Chua, L.P., 1989. Calibration of X-probes for turbulent flow measurements. Experiments in Fluids 7, 201–208.

Cutler, A.D., Bradshaw, P., 1993a. Strong vortex/boundary layer interactions, Part 1, vortices high. Experiments in Fluids 14, 321–332.

Cutler, A.D., Bradshaw, P., 1993b. Strong vortex/boundary layer interactions, Part 1, vortices low. Experiments in Fluids 14, 393–401.

Eckelmann, H., Kastrinakis, E., Nychas, S.G., 1984. Vorticity and velocity measurements in a fully developed turbulent channel flow. In: Tatsumi T. (Ed.), Turbulent and chaotic phenomena in fluids, Proceedings of the IUTAM Symposium, Kyoto 1983, North-Holland, pp. 421–426.

Eckelmann, H., 1997. Einführung in die Strömungsmesstechnik. Teubner, Stuttgart, Germany.

Eibeck, P.A., Eaton, J.K., 1985. An experimental investigation of the heat transfer effects of a longitudinal vortex embedded in a turbulent boundary layer. Rept. MD-48, Thermosciences Division, Department of Mechanical Engineering, Stanford Unversity.

Eibeck, P.A., Eaton, J.K., 1986. The effects of longitudinal vortices embedded in a turbulent boundary layer on momentum and thermal transport. Proceedings of the Eighth International Conference on Heat Transfer, vol. 3, pp. 1115–1120.

Eibeck, P.A., Eaton, J.K., 1987. Heat transfer effects of a longitudinal vortex embedded in a turbulent boundary layer. Transactions of the ASME, vol. 109.

Klick, H., 1992. Einfluss variabler Stoffwerte bei der turbulenten Plattenstromung. Fortschrittberichte VDI, Reihe 7: Strömungstechnik, 213 VDI-Verlag, Düsseldorf.

Kline, S.J., 1985. The purposes of uncertainty analysis. Journal of Fluids Engineering 107, 153–160.

Kostka, M., Vasanta Ram, V.I., 1992. On the effect of fluid temperature on hot-wire characteristics, Part 1: Results of experiments. Experiments in Fluids 13, 155–162.

Lau, S., Schulz, V., Vasanta Ram, V.I., 1993. A computer operated traversing gear for three-dimensional flow surveys in channels. Experiments in Fluids 14, 475–476.

Lau, S., 1995. Experimental study of the turbulent flow in a channel with periodically arranged longitudinal vortex generators. Experimental Thermal and Fluid Sciences 11 (3), 225–261.

Lau, S., 1996. Messung und Analyse der Transportgrössen in der turbulenten Kanalströmung mit eingebetteten Längswirbeln. Dr.-Ing. Thesis, Fakultat für Maschinenbau, Ruhr University Bochum, 44780 Bochum, Germany.

Lau, S., Vasanta Ram, V., 1998. Measurement and analysis of the turbulent flow quantities in a channel with embedded longitudinal vortices. In: Mitra, N.K., Fiebig, M. (Eds.), Notes on Numerical Fluid Mechanics. Vieweg, Braunschweig and Wiesbaden, Germany, vol. 63, pp. 252–287.

Meyer, L., 1994. Measurements of turbulent velocity and temperature in axial flow through a heated rod bundle. Nuclear Engineering and Design 146, 71–82.

Moffat, R.J., 1985. Using uncertainty analysis in the planning of an experiment. Journal of Fluids Engineering 107, 173–182.

Neumann, H., 1997. Experimentelle Untersuchung von hydrodynamischen und thermischen Anlaufströmungen mit periodisch angeordneten Wirbelerzeugern. Dr.-Ing. Thesis, Fakultät für Maschinenbau, Ruhr University Bochum, 44780 Bochum, Germany.

Neumann, H., Braun, H., Fiebig, M., 1998. Vortex structure, Heat transfer and flow losses in turbulent channel flow with periodic longitudinal vortex generators. In: Mitra, N.K., Fiebig, M. (Eds.), Notes on Numerical Fluid Mechanics. Vieweg, Braunschweig and Wiesbaden, Germany, vol. 63, pp. 288–327.

Park, S.R., Wallace, J.M., 1992. The influence of velocity gradients on turbulence properties measured with multi-sensor hot-wire probes. Thirteenth Symposium on Turbulence, 21–23 September, 1992, Rolla, MO, USA.

Praisner, T.J., Seal, C.V., Takmaz, L., Smith, C.R., 1997. Spatial-temporal turbulent flow-field and heat transfer behaviour in end-wall junctions. International Journal of Heat and Fluid Flow 18 (1), 142–151.

Riemann, A., 1992. Waermeuebergang und Druckabfall in Kanaelen-mit periodischen Wirbelstroemungen bei thermischen Anlauf. Dr.-Ing. Thesis, Fakultät für Maschinenbau, Ruhr University Bochum, 44780 Bochum, Germany.

Schulz, V., 1989. Der Wellencharakter der Turbulenzstruktur einer ebenen, raeumlich gestoerten Kanalstroemung. Fortschrittberichte VDI, Reihe, 7: Stromungstechnik, vol. 153, VDI-Verlag, Düsseldorf, Germany.

Shabaka, I.M.M.A., Mehta, R.D., Bradshaw, P, 1988. Longitudinal vortices imbedded in turbulent boundary layers. Part 1: Single vortex. Journal of Fluid Mechanics 155 (1), 37–57.

Shizawa, T., Eaton, J.K., 1992. Turbulence measurements for a longitudinal vortex interacting with a three-dimensional turbulent boundary layer. AIAA Journal 30 (1), 49–56.

Townsend, A.A., 1976. The Structure of Turbulent Shear Flow, 2nd ed. Cambridge University Press, Cambridge.

Vasanta Ram, V., 1992. On the effect of fluid temperature on hot-wire characteristics. Foundations of a rational theory. Experiments in Fluids 13 (2), 267–278.

Wittmer, K.S., Davenport, W.J., Zsoldos, J.S., 1998. A four-sensor hot-wire system for three-component velocity measurement. Experiments in Fluids 23, 416–423.

Wroblewski, D.E., Eibeck, P.A., 1991. Measurements of turbulent heat transport in a boundary layer with an embedded streamwise vortex. International Journal of Heat and Mass Transfer 34 (7), 1617–1631.

Xie, Q., Wroblewski, D., 1997. Effect of periodic unsteadiness in heat transfer in a turbulent boundary layer downstream of a cylinder-wall junction. International Journal of Heat and Fluid Flow 18 (1), 107–115.

Zhu, J.X., 1992. Wärmeübergang und Strömungsverlust in turbulenten Spaltströmungen mit Wirbelerzeugern. Fortschrittberichte VDI, Reihe, 7: Strömungstechnik, vol. 192, VDI-Verlag, Düsseldorf, Germany.

Zhu, J.X., Mitra, N.K., Fiebig, M., 1991. Numerical simulation of periodically fully developed turbulent flow and heat transfer in a channel with longitudinal vortex generators. Eighth Symposium on Turbulent Shear Flows, 9–11 September, 1991, Munich, Germany.